CrossMark

Impacts of SST Warming in tropical Indian Ocean on CMIP5 model-projected summer rainfall changes over Central Asia

Yong Zhao[1] · Huqiang Zhang[2]

Abstract Based on the *historical* and *RCP8.5* experiments from 25 Coupled Model Intercomparison Project phase 5 (CMIP5) models, the impacts of sea surface temperature (SST) warming in the tropical Indian Ocean (IO) on the projected change in summer rainfall over Central Asia (CA) are investigated. The analysis is designed to answer three questions: (1) Can CMIP5 models reproduce the observed influence of the IO sea surface temperatures (SSTs) on the CA rainfall variations and the associated dynamical processes? (2) How well do the models agree on their projected rainfall changes over CA under warmed climate? (3) How much of the uncertainty in such rainfall projections is due to different impacts of IO SSTs in these models? The *historical* experiments show that in most models summer rainfall over CA are positively correlated to the SSTs in the IO. Furthermore, for models with higher rainfall-SSTs correlations, the dynamical processes accountable for such impacts are much closer to what have been revealed in observational data: warmer SSTs tend to favor the development of anti-cyclonic circulation patterns at low troposphere over north and northwest of the Arabian Sea and the Bay of Bengal. These anomalous circulation patterns correspond to significantly enhanced southerly flow which carries warm and moisture air mass from the IO region up to the northeast. At the same time, there is a cyclonic flow over the central and eastern part of the CA which further brings the tropical moisture into the CA and provides essential moist conditions for its

rainfall generation. In the second half of twenty-first century, although all the 25 models simulate warmed SSTs, significant uncertainty exists in their projected rainfall changes over CA: half of them suggest summer rainfall increases, but the other half project rainfall decreases. However, when we select seven models out of the 25 based on their skills in capturing the dynamical processes as observed, then the model projected changes are much closer. Five out of the seven models predicted more rainfall over CA. Such a result is helpful for allowing us to attribute part of the observed upward rainfall trend in the CA region in the last several decades to the IO SST warming.

1 Introduction

The central Asia (CA) is one of the largest arid and semi-arid areas in the world, with an area over 4×10^6 km^2, across Kazakhstan, Kyrgyzstan, Tajikistan, Turkmenistan, and Uzbekistan and part of northwest China (Huang et al. 2014). In CA, water is particularly scarce and its ecosystems, economy and society are extremely venerable to the variations of rainfall received. Yet, its climate is highly sensitive to global climate change (Huxman and Smith 2001; Whitford 2002). Some studies argued that CA maybe one of the regions which is likely to be strongly affected by global warming (Solomon et al. 2007; Chen et al. 2009).

Indeed, there are studies showing some remarkable regional features of observed climate changes in CA. Chen et al. (2009) showed that the observed warming intensity in CA exceeds the averaged surface temperature changes over the Northern Hemisphere during the

✉ Yong Zhao
zhaoyong@idm.cn

[1] Institute of Desert Meteorology, China Meteorological Administration, Ürümqi, Xinjiang, China

[2] Bureau of Meteorology, Melbourne, VIC, Australia

 Springer

past 100 years. Furthermore, recent studies showed that its annual rainfall is enhanced in the last several decades. This is contradictory to the drying trend over the subtropical land regions projected by climate models (Chen et al. 2011; Huang et al. 2012). Several studies documented in details that in the Xinjiang province in northwest China, which is located in the eastern part of CA, its summer rainfall has experienced significant decadal changes and such changes are different from the changes occurred in eastern China (Shi et al. 2002). Nevertheless, studies focusing on questions such as how and why the rainfall changes in the region in past and future climate are still very limited. This has become the purpose of this study which is aimed to explore three questions: (1) Can current climate models reproduce the observed rainfall changes over CA and the associated dynamical processes? (2) How well do the models agree on their projected rainfall changes over CA under warmed climate? (3) How large is the uncertainty in rainfall projections from current climate modeling experiments and what are the likely reasons leading to this?

It is well known that tropical oceans are one of the fundamental drivers of the global climate. Inthe past several decades, observations have shown that global oceans become warmer (Zeng et al. 2001; Gille 2002; Levitus et al. 2005). In particular, the whole Indian Ocean (IO) has experienced significant warming during the last half century (Chambers et al. 1999; Alory et al. 2007; Du and Xie 2008). Some studies even claimed that the SST warming in IO was the strongest and most robust warming signal among the global oceans (Lau and Weng 1999; Hoerling et al. 2004). Many studies have demonstrated that the warming in IO not only has dominant effects in south Asian monsoon regime but also can have far-reaching impacts on regions including Asia, Africa and Australia (Clark et al. 2000; Ashok et al. 2001; Giannini et al. 2003; England et al. 2006).

Furthermore, recent studies showed that the IO SSTs can affect large-scale circulations which are closely related to rainfall over CA. For instance, Kawamura (1994) showed that the SSTs anomalies in IO can influence climate variability in middle latitude of Asia. Correlations analysis found the summer rainfall in east part of CA has a close relationship with the spring and summer SSTs in the IO (Yang et al. 2010; Zhou et al. 2015). Composite analysis showed that summer rainfall in the east part of CA increased during the years of earlier onsets of the south Asian summer monsoon (Xu and Qian 2006). Studies also showed that rainfall over central and southwest Asia is also derived from tropical moisture sources and is well associated with tropical climate variability (Mason and Goddard 2001; Mariotti et al. 2005). Statistical results showed that

water vapor from the IO plays an important role in generating summer rainfall over east part of CA, especially in heavy rainfall (Yang and Zhang 2007; Bothe et al. 2012; Zhao et al. 2014).

It is widely acknowledged that large uncertainty exists in current climate model rainfall projection at regional scales. There are a limited number of studies focusing on the potential changes in the summer rainfall over CA under global warming. Based on the outputs from a few selected CMIP5 models, Wu et al. (2013) and Huang et al. (2014) reported significant uncertainties in the model–projected rainfall changes over CA. After selecting a few models with relatively good skills for simulating current rainfall climatology, they reported future rainfall increases across most part of CA in these models. However, it is yet unclear the causes of such rainfall increases and to what extent they are related to the warming in the IO. The current climate projections tend to suggest that the Asian monsoon circulations are to be weakened under global warming (Fan et al. 2010, 2012; Sooraj et al. 2014). Thus, it is not well understood about the combined effects from a warmed IO and a weakened tropical monsoon circulation on the potential rainfall responses over CA. Although observational analysis showed that a weakened south Asian summer monsoon could result in the cooling in middle and upper troposphere over CA and furthermore generate favorable anomalous circulations for generating more summer rainfall in east part of CA (Yang et al. 2009; Zhao et al. 2014), we do not know if the same processes operate in the models.

Therefore, in this study, we first evaluate the skill of current climate models in reproducing the dynamical processes of how the tropical IO SSTs affect the rainfall over CA. Then we assess if the models can reproduce the linkage between the warming in the IO and the rainfall increases over CA. Following these evaluations, we then select models to assess if the models with reasonable skill in capturing these fundamental observed features can offer reasonable agreement in their projected changes of rainfall over CA. Accordingly, the manuscript is arranged as follows: the descriptions of observational and modeling data used in this study are given in Sect. 2. The model-simulated relationship between summer rainfall across CA and SSTs in the IO is evaluated in Sect. 3. The projected changes in summer rainfall over CA and its response to the IO warming are shown in Sect. 4. Results from a climate model's SST sensitivity experiments are also included in the analysis to examine the processes identified in the CMIP5 model results. Section 5 summarizes the main conclusions from this study and discusses the weakness and further work needed to strengthen our further understanding of the climate and its projects in CA.

2 Datasets used in the analysis

The datasets used in this study are shown as follows:

(1) Observational data: As high quality observed rainfall and temperature station data over CA are not readily available, in this study we use the Climate Research Unit (CRU) version 3.10 monthly data which covers global land with a horizontal resolution of $0.5° \times 0.5°$ (Mitchell and Jones 2005). This data is widely used in climate and climate change studies (Houghton et al. 2001; Jone et al. 2001). In this analysis, SST data for the period of 1959–2004 come from the monthly $2° \times 2°$ SSTs by Reynolds et al. (2002) of the US National Oceanic and Atmospheric Administration (NOAA). The ERA-40 reanalysis (Uppala et al. 2005) during 1959–2001is used to reveal the large-scale atmospheric circulation patterns responsible for the impacts of IO SSTs on CA climate. We have re-examined the results using the National Centers for Environment Prediction (NCEP)/National Center for Atmospheric Research (NCAR) reanalysis dataset (Kalnay et al. 1996) and results show very similar features and therefore not reported here.

(2) Climate model data: Monthly precipitation, surface temperature, zonal and meridional winds from *historical* and *RCP8.5* experiments of 25 CMIP5 coupled climate models (Table 1) are used in this study. These are the models used in the analysis of Dong et al. (2015) and Zhang et al. (2015) in which they assessed the CMIP5 model-simulated changes in the onset/retreat of the Australia–Asian monsoon. When designing the study, we used the same models for allowing us to potentially link changes in tropical monsoon climate with rainfall changes over CA. The model outputs from the *historical* and *RCP8.5* experiments for the periods of 1961–2004 and 2051–2100 are used in this analysis. For all models and experiments, only one ensemble run is used and the model outputs are interpolated onto the same horizontal resolution of $1.5° \times 1.5°$ using a bilinear interpolation method. More details about the experimental designs of the *historical* and *RCP8.5* experiments can be found in Taylor et al. (2012).

To support our analysis of the CMIP5 model results, we have conducted a set of SST sensitivity experiments using one of the CMIP5 model (ACCESS1.3, Bi et al. 2013). The model details are readily available in the CMIP5 model

Table 1 The 25 CMIP5 models used in the analysis

| Model		AGCM horizontal/vertical resolution
ACCESS1-0	CAWCR, Australia	1.9×1.2 L38
ACCESS1-3	CAWCR, Australia	1.9×1.2 L38
bcc-csm1-1	BCC, CMA, China	2.8×2.8 L26
bcc-csm1-1-m	BCC, CMA, China	2.8×2.8 L26
BNU-ESM	BNU, China	2.8×2.8 L26
CanESM2	CCCMA, Canada	2.8×2.8 L35
CMCC-CM	CMCC, Italia	0.75×0.75 L31
CMCC-CMS	CMCC, Italia	0.75×0.75 L31
CNRM-CM5	CNRM-CERFACS, France	1.4×1.4 L31
CSIRO-Mk3-6-0	CSIRO-QCCCE, Australia	1.9×1.9 L18
FGOALS-s2	LASG-CESS, China	2.8×1.7 L26
GFDL-CM3	NOAA-GFDL, USA	2.5×2.0 L48
GFDL-ESM2G	NOAA-GFDL, USA	2.5×2.0 L24
GFDL-ESM2M	NOAA-GFDL, USA	2.5×2.0 L24
HadGEM2-CC	MOHC, UK	1.9×1.2 L60
inmcm4	INM, Russia	2.0×1.5 L21
IPSL-CM5A-LR	IPSL, France	3.7×1.9 L39
IPSL-CM5A-MR	IPSL, France	2.5×1.3 L39
IPSL-CM5B-LR	IPSL, France	3.7×1.9 L39
MIROC5	AORI-NIES-JAMSTEC, Japan	1.4×1.4 L40
MIROC-ESM	AORI-NIES-JAMSTEC, Japan	2.8×2.8 L80
MIROC-ESM-CHEM	AORI-NIES-JAMSTEC, Japan	2.8×2.8 L80
MPI-ESM-LR	MPI-N, Germany	1.9×1.9 L47
MPI-ESM-MR	MPI-N, Germany	1.9×1.9 L95
MRI-CGCM3	MRI, Japan	1.1×1.1 L31
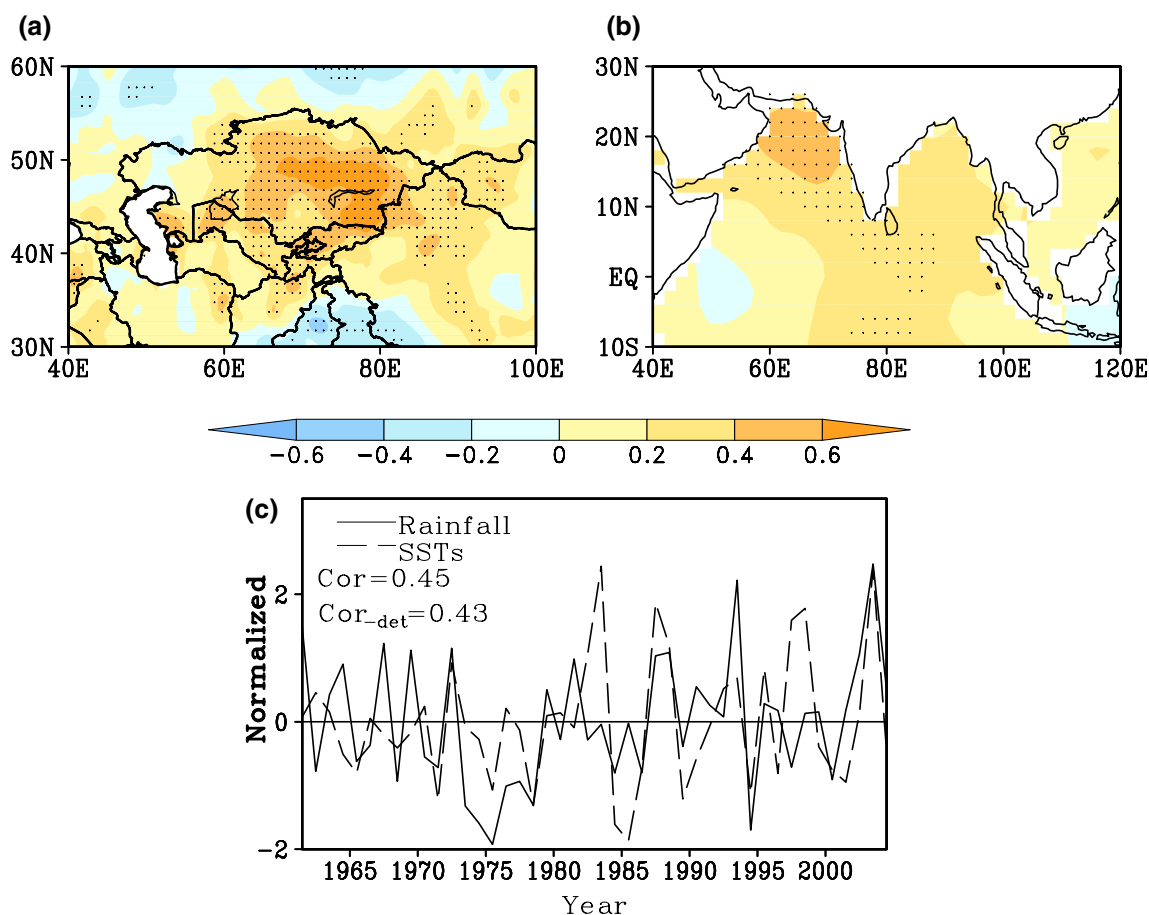
Fig. 1 **a** Correlations between regionally averaged rainfall over the domain of 73–95°E, 35–50°N and rainfall over central Asia in summer, **b** correlations between regionally averaged rainfall from the domain of 65–95°E, 35–50°N and SSTs in Indian Ocean in summer, **c** interannual variations of summer rainfall averaged over the domain of 65–95°E, 35–50°N during 1961–2004 and SSTs averaged over the domain of 50–75°E, 5–25°N during 1961–2004, together with correlations between the two with/without detrended data

documentation. Here we only brief three AMIP-type SST experiments conducted using the atmospheric model of ACCESS1.3: ACCESS-his uses the global SSTs simulated from the coupled ACCESS1.3 CMIP5 *historical* experiments for the period of 1971–2000; in ACCESS-rcp85 we super-impose the ACCESS1.3 fully coupled model-simulated changes in global SSTs by its *RCP8.5* experiment for the period of 2071–2100 onto the ACCESS-his, together with changes in atmospheric greenhouse gases as in *RCP8.5*; ACCESS-no IO uses the same SST warming as in ACCESS-rcp85 but with no warming over the tropical IO (with a domain of 20°S–30°N, 40–100°E). ACCESS-only IO uses the SST warming as in ACCESS-rcp85 but SST warming only occurring over the IO. These experiments help us to examine whether IO warming contributes to the rainfall increases in the CA.

Summer is the main rainy season in most part of the CA. It accounts for a large proportion of its annual rainfall totals. For example, in the east part of CA the summer rainfall can accounts for 40–50 % of annual rainfall received

(Zhang and Deng 1987). So in current study, we only focus on analyzingresults in the boreal summer season June–July–August (JJA).

3 Observed and model-simulated linkages between IO SSTs and CA rainfall

Complex terrains occupy the CA region, including high mountain ranges and flat plains. Prior to the analysis, we firstly assess the spatial homogeneity of summer rainfall variations in the CA domain. Figure 1a shows the correlations of area-averaged rainfall over eastern part of the CA (with the domain of 73–95°E, 35–50°N) and rainfall over the whole CA during 1961–2004. Positive correlations occupy most of the region, and high correlations are largely located in the domain of 65–95°E, 35–50°N where the zonal westerly dominates (Lioubimtseva et al. 2005). Above result suggests the summer rainfall variations are by and large homogeneous in space across most of the

CA despite of regional contrasts in their long term means. Based on the results above, we now define a summer precipitation index (SPI) over CA as regionally averaged summer rainfall over the domain of 65–95°E, 35–50°N.

Figure 1b shows the SPI correlations to SSTs in the tropical IO, with statistically significant results being marked. It illustrates that the SPI is well correlated to the SSTs in tropical IO. The correlations are higher in the Arabian Sea than in the Bay of Bengal. This is consistent with other observational analyses (e.g., Yang et al. 2010). Furthermore, Fig. 1c shows the times series of the interannual variations of summer rainfall averaged over the domain of 65–95°E, 35–50°N over CA and SSTs averaged over the domain of 50–75°E, 5–25°N in IO during 1961–2004. Clearly, summer rainfall over CA is closely linked to the SSTs in the tropical IO, with the two having a correlation of 0.45. Although the figure exhibits rainfall increasing trend since the late 1970s when the IO experiences substantial warming, the correlation does not reduce much after removing the long term trends in these time series (with correlation coefficient being 0.43 with detrended data). This suggests the linkage between the two is strong at both interannual and decadal time scales.

How do the SST anomalies in the IO influence the summer rainfall over CA? Previous studies suggested that this is largely through the atmospheric circulation responses to the SST anomalies in the tropics (Zhao et al. 2014; Zhou et al. 2015). Here, we examine the likely underlying processes by asking two questions: how IO SSTs affect the regional circulations which determine the dynamical conditions for rainfall generation; the other is how IO SSTs affect the atmospheric moisture condition which is the thermodynamic condition for rainfall generation. First of all, Fig. 2a displays the correlations of regionally averaged SSTs of Reynolds et al. (2002) over the domain of 50–75°E, 5–25°N in the IOas in Fig. 1c and the horizontal wind averaged between 850 and 700 hPa (representing the lower tropospheric circulation) in the ERA-40 reanalysis data. It also shows the horizontal convergence calculated from the wind correlations with the SSTs. It is obvious that there are significant atmospheric responses to the SSTs in the Arabian Sea region. Warmer SSTs there are favorable for the formation of a strong cyclonic circulation, enhanced low-level convergence and therefore strengthened upward motion in the tropical IO region. This suggests SSTs are the driving force for the atmospheric dynamics in the domain, rather than being passive responses to atmospheric forcing. To its north, there is a giant anti-cyclonic flow anomaly over the domain around 20–30°N and 35–70°E. The anti-cyclonic system can largely be viewed as the corresponding descending branch of the enhanced ascending motion in the tropical IO. This anomalous pattern corresponds to a significantly enhanced southerly flow over the longitudinal band
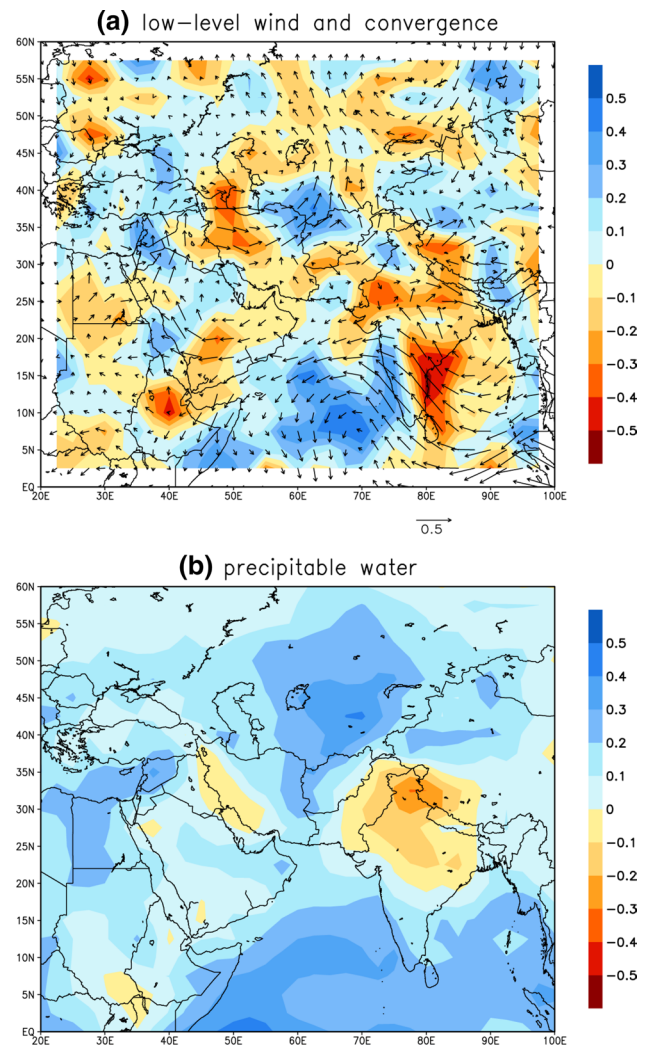

Fig. 2 a Low-level wind (averaged between 850 and 700 hPa) from ERA-40 reanalysis data (Uppala et al. 2005) for the period of 1959–2001 correlating to the same IO SST index defined in Fig. 1c. *Shaded colours* are the horizontal convergence calculated from the wind and SST correlations, **b** correlations between the IO SST index with the volumetrically integrated precipitable water from ERA-40 reanalysis for the same period

of 35–45°E. In the eastern part of the tropical domain, one can be seen a strong anti-cyclonic pattern occupying most of the Indian subcontinent, the Bay of Bengal and to the south of the Tibetan Plateau. Associated with this pattern, a strong southerly flow dominates the subcontinent and extending further north up to the low-land region between the Iranian Plateau and Tibetan Plateau. Together, these two enhanced southerly branches are important for conveying tropical moisture into the subtropical region. Although big terrains block the moist air in the east of 70°E, Zhao et al. (2014) showed that in between the Tibetan Plateau and the Iranian Plateau most part of valley is below 1500 m and the southerly anomalies can transport the moist air into CA

through this valley. To the north of these two anti-cyclonic patterns, there is a cyclonic pattern around the domain of 30–50°N and 40–65°E. The anomalous southwesterly wind associated with the trough pattern over CA can further transport the moist air originated from the IO into CA for generating more summer rainfall. This is the so-called two-step process as revealed in Zhao et al. (2014).

Figure 2b further shows the correlations between volumetrically integrated atmospheric precipitable water from the ERA-40 reanalysis to the same area-averaged SSTs used in Fig. 2a. Associated with the SST warming in the Arabian Sea region, the atmosphere is further moistened in the CA region. The agreement between circulation patterns in Fig. 2a and the moisture conditions in Fig. 2b is reasonably well, suggesting the moistening process can be attributed to direct consequences of the atmospheric circulation responses to the SST forcing in the IO. Furthermore, over CA, not only is the atmospheric moisture condition much improved (Fig. 2b), but also the low-level convergence is strengthened (Fig. 2a) corresponding to the cyclonic circulation pattern over CA. Such a nice combination of improved dynamical and moisture conditions leads to high correlations between IO SSTs and CA rainfall as revealed in Fig. 1.

Our analysis is consistent with many previous studies on the important role of IO SSTs on CA rainfall. Synoptic analysis from Zhang et al. (2012) showed that two classic synoptic situations corresponding to Xinjiang rainfall generation: either (1) the trough embedded in the middle latitude westerly is deep enough extending far southward to bring tropical moist air into the CA region; or (2) the middle latitude trough is supported by another subtropical system which is able to transport the tropical moist air into the middle latitude trough region. There are plenty of trough/ridge developments along the middle latitude westerly due to the baroclinic nature of the atmosphere in the region, but it is moisture condition limiting the summer rainfall received. This is the reason why throughout this analysis, we focus on the moisture source in explaining rainfall variations and changes in CA. Following the observational analysis, we now use such information to assess whether CMIP5 models can reproduce such a connection between IO SSTs and summer rainfall over CA and the associated processes shown in Figs. 1 and 2. Figure 3 shows the correlations of regionally averaged rainfall from the eastern part of CA (the domain of 73–95°E, 35–50°N) and rainfall across a much larger CA domain in the 25 models in their *historical* runs (1961–2004). Positive correlations occupy most part of the CA in a majority of the models, which are similar to Fig. 1a. High correlations are roughly located in the domain of 65–95°E, 35–50°N as observed (Fig. 1a).

Furthermore, in order to assess the model-simulated relationship between summer rainfall over CA and IO SSTs, Fig. 4 gives the correlations of regionally averaged summer rainfall over the domain of 65–95°E, 35–50°N and SSTs in IO. Again, statistically significant correlations are highlighted in the figures. Although a large number of the models show some positive correlations, the magnitude of such correlations varies significantly across the models. Such cross-model variations could have significant implications on their projections of the changes in CA rainfall under global warming which will be discussed in the following section. In addition, the correlation is generally higher in the Arabian Sea than in the Bay of Bengal. This is also seen in Fig. 1b. Therefore, in the following analysis, we will mainly focus on the analysis of SSTs in the Arabian Sea.

Above results only give the correlations of regionally averaged summer rainfall over the domain of 65–95°E, 35–50°N and SSTs in IO. It is likely that some models may have some skill in simulating such a linkage but the location of high rainfall-SST correlations may be away from the domain selected in Fig. 4. Thus, to give a more comprehensive picture about the connections between SSTs in the IO and rainfall over CA, Fig. 5 displays the correlations of regionally averaged SSTs from the domain of 50–75°E, 5–25°E in the Arabian Sea and summer rainfall over a much larger domain over CA. Indeed, in most models, high correlations are all located in the domain of 65–95°E, 35–50°N which are quite consistent with the distribution in Fig. 1a. Nevertheless, the extent of such correlations varies among the models, with some models giving much higher correlations than others.

To further examine if the rainfall-SSTs correlations in the models are caused by the same processes identified in the observational results in Fig. 2, we have calculated the correlations between regionally averaged SSTs from the domain of 50–75°E, 5–25°E in the Arabian Sea and the horizontal wind averaged between 850 and 700 hPa as used in Fig. 2a. We found (not shown) that in the 25 models, their skills in reproducing the dynamical processes identified in Fig. 2 vary significantly. Some of them show reasonable skills, while others give large differences from observed results.

To objectively quantify the model skills in reproducing the connections between IO SSTs and CA rainfalls and the underlying processes, we have combined two measurements in our model selecting exercise: one is the correlation between CA rainfall and SSTs over 50–75°E, 5–25°N as shown in Fig. 1c, and the other is the correlation between the same SSTs data with the meridional wind component in the area of 15–30°N, 35–45°E where in Fig. 2a we can see significant circulation signal responding to the IO SSTs conditions. Figure 6 shows the correspondences between the two correlation coefficients in each of
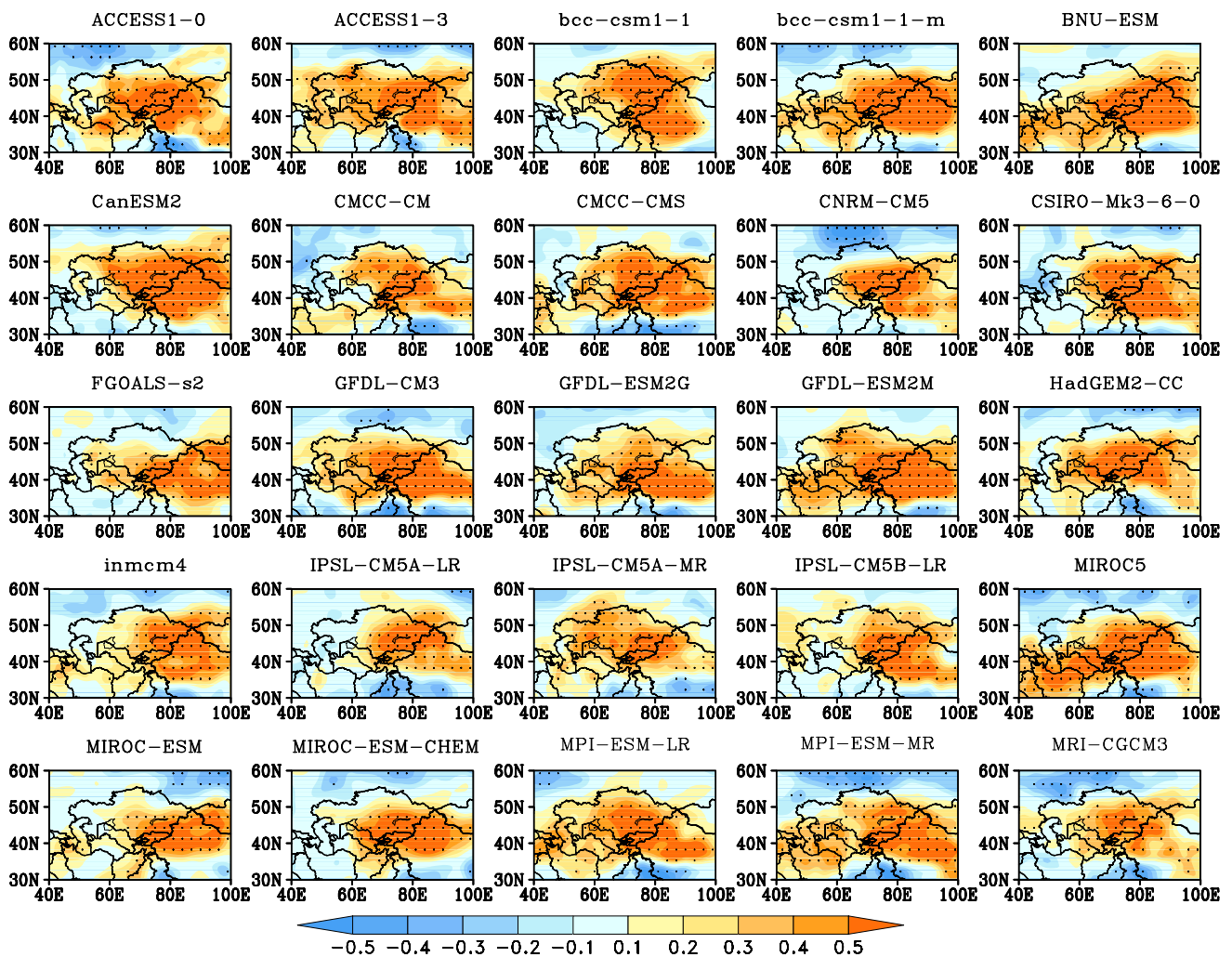
Fig. 3 Correlations between regionally averaged rainfall from the domain of 73–95°E, 35–50°N and rainfall over central Asia in JJA in 25 CMIP5 models' historical run for the period of 1961–2004. Statistically significant results at 95 % confidence level are marked by *dot points*

the 25 models. We have found out of the 25, seven models are able to reproduce statistically significant correlations as observed in Figs. 1 and 2. These models are BNU-ESM, CanESM2, CMCC-CMS, GFDL-ESM2M, IPSL-CM5B-LR, MIROC5 and MPI-ESM-MR. Some of the models in our selection have also been selected in Huang et al. (2014) in which they selected CMIP5 models based on their skills of reproducing observed rainfall mean climatology, rather than on the processes governing the rainfall variations as applied in this analysis.

In Fig. 7, it is obvious that these seven models, by and large, show overall circulation patterns as observed (Fig. 2a). Anti-cyclonic flow patterns seen in Fig. 2a over north Arabian Sea and its northwest and over the Bay of Bengal region, to a varying extent, are presented in these model results. The ensemble averages from the seven models offer satisfactory agreement with the patterns

shown in Fig. 2a. Nevertheless, there are some notable inter-model differences. In the CanESM2 model, the cyclonic flow over CA region is not as clear as seen in other models. The results from GFDL-ESM2M to MPI-ESM-MR are largely similar to others but over the Bay of Bengal, there is an anomalous cyclonic pattern instead. The MPI-ESM-MR also shows relatively weak cyclonic flow patterns over CA. In the MIROC5 model anomalous anticyclones present over north Arabian Sea and Bay of Bengal, but its location is further northward. Despite of these inter-model differences, the 7-model ensemble results in Fig. 7 illustrate the overall following common features: over tropical IO, there is an enhanced cyclonic flow patterns. To its north, anti-cyclonic flow patterns correspond to enhanced southerly flow which carries warm and moist air north of the IO. At the same time, there is a cyclonic anomaly over CA which can further transport
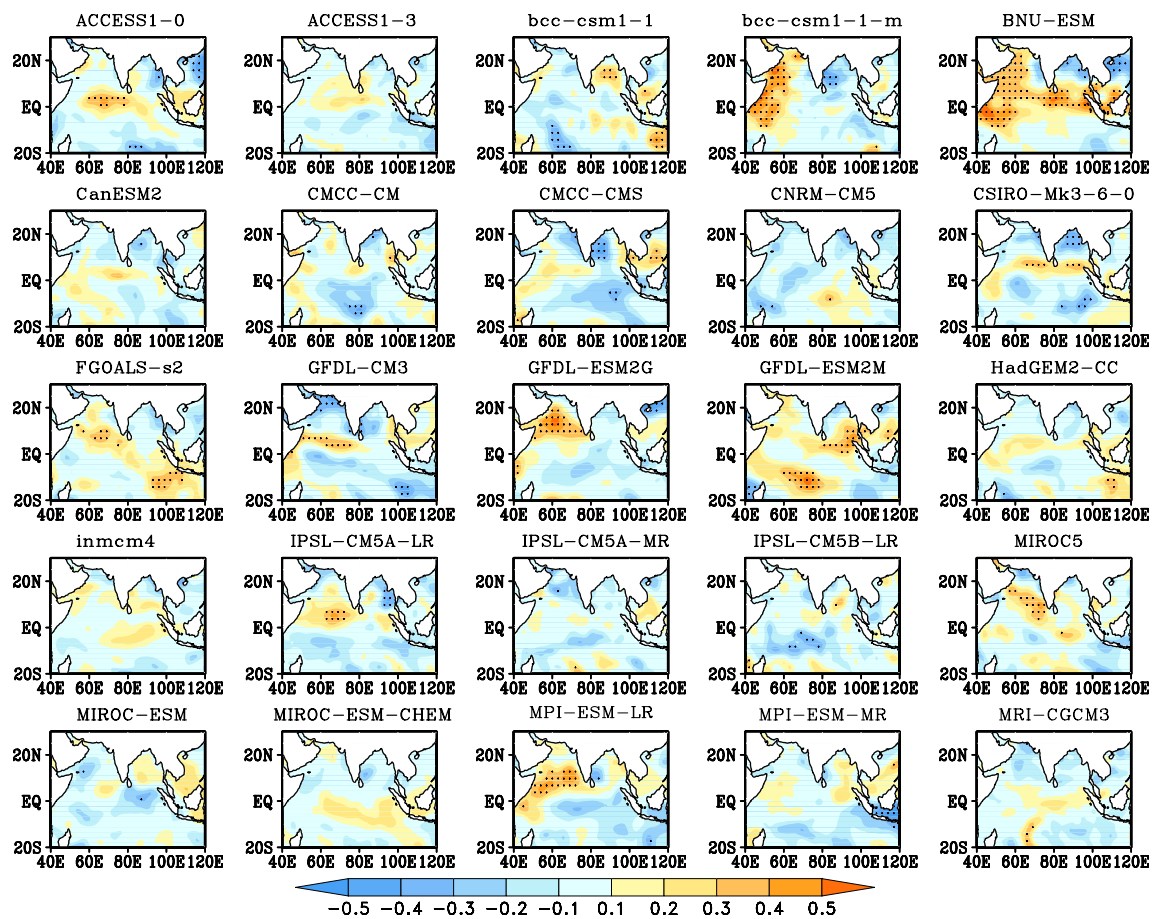
Fig. 4 As Fig. 3, but for correlations between regionally averaged rainfall from the domain of 65–95°E, 35–50°N and SSTs in Indian Ocean

such tropically originated moisture into the CA region and favor rainfall generation. They are in good agreement with observational results presented in Fig. 2 and other studies (e.g., Zhao et al. 2014).

4 Projected change in summer rainfall over CA

In Sect. 3, we have focused on assessing the CMIP5 model skills in reproducing the observed influence of SSTs in tropical IO (in particular over the Arabian Sea) on the CA summer rainfall and the underlying processes. In this section, we analyze the model-projected changes in future and uncertainties in these projections. Several recent studies suggested that rainfall over CA may continue to increase in the twenty-first century based on the model outputs from CMIP5 (Wu et al. 2013; Huang et al. 2014), but less attention has been paid to explore the mechanisms leading to such projected changes. Besides, none of these studies have investigated the likely causes of uncertainty in these models. Here, we concentrate our analysis on the linkages between IO SST warming, tropical monsoon circulation

changes and rainfall responses over CA under greenhouse warmed climate.

As one can expect, Fig. 8 shows that all the models simulate SST warming in IO under the global warming. However, the SST warming is not uniform in the Arabian Sea and Bay of Bengal. The SST warming in Arabian Sea is stronger than in the Bay of Bengal in most models. This is consistent with the observed changes in the IO in the last several decades (Roxy et al. 2014). We now explore whether these can be used to explain the model-projected changes in rainfall.

Figure 9a displays the projected change in summer rainfall over CA (averaged over the domain of 65–95°E, 35–50°N) from the 25 models between the rainfall climatology averaged over 2051–100 in their *RCP8.5* runs against the one derived from their *historical* runs over the period of 1961–2004. Despite of the warmed IO in all the models, changes in summer rainfall show remarkable differences among the models. For the 25 models, 14 of them show increased summer rainfall while the other 11 models suggest rainfall decreases. If one does not separate these models in terms of their skills in simulating the processes affecting summer rainfall over
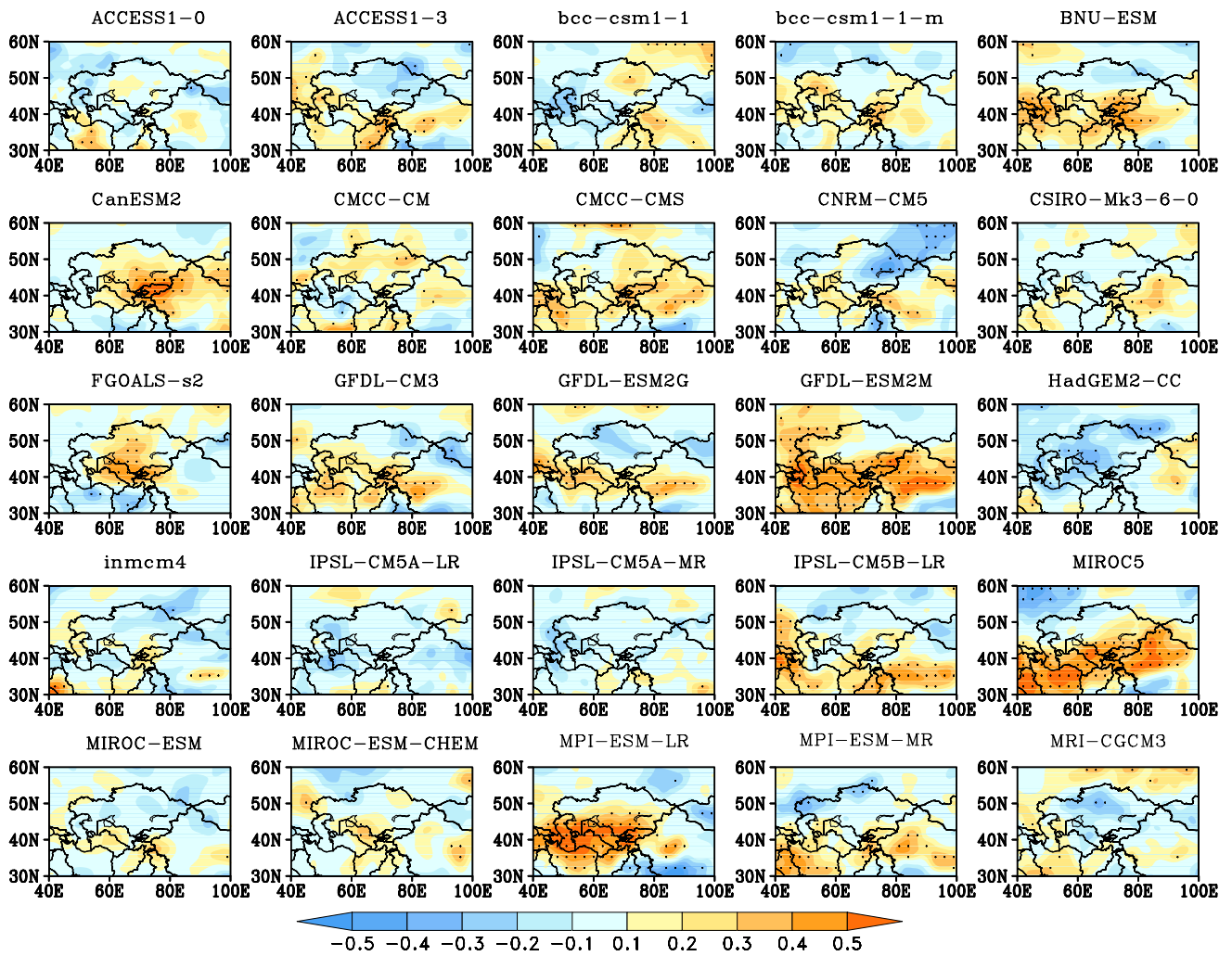
Fig. 5 As Fig. 3, but for correlations between regionally averaged SSTs from the domain of 50–75°E, 5–25°N and rainfall over central Asia
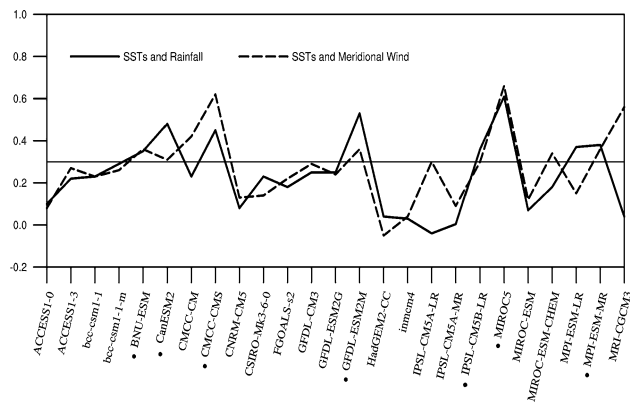

Fig. 6 *Solid line* shows the correlations between summer rainfall averaged over the domain of 65–95°E, 35–50°N and SSTs averaged over the domain of 50–75°E, 5–25°N in the 25 CMIP5 models' *historical* experiment for the period of 1961–2004, *Dashed line* shows the correlations between SSTs averaged over the domain of 50–75°E, 5–25°N and the meridional wind component in the area of 15–30°N, 35–45°E. Seven models marked by *dots* are the ones showing both positive correlations passing 95 % confidence level

CA, a simple multi-model ensemble average yields a very weak change due to the offsetting results among the models. Such results are very misleading. In contrast, using the seven models selected in Sect. 3, such uncertainty becomes much smaller. Five out of the seven models show the summer rainfall will increase, with only two models (CMCC-CMS and MPI-ESM-MR)) showing much weaker decreases (Fig. 9b). Based on the fact that these models have reasonable skill in reproducing the important process of IO SSTs in modulating the rainfall in CA, results derived from such models are more convincing and reliable.

Figure 10 further shows the spatial features of the changes in summer rainfall over CA in the seven selected models. Five of the seven models illustrate overall rainfall increases over CA region, particularly over a large part of the Xinjiang Province in northwest China (about 73–95°E, 35–50°N). Most of the changes are statistically significant with *t* test. Note that although the magnitude of these changes is small, they are huge changes in terms of percentage to the very low
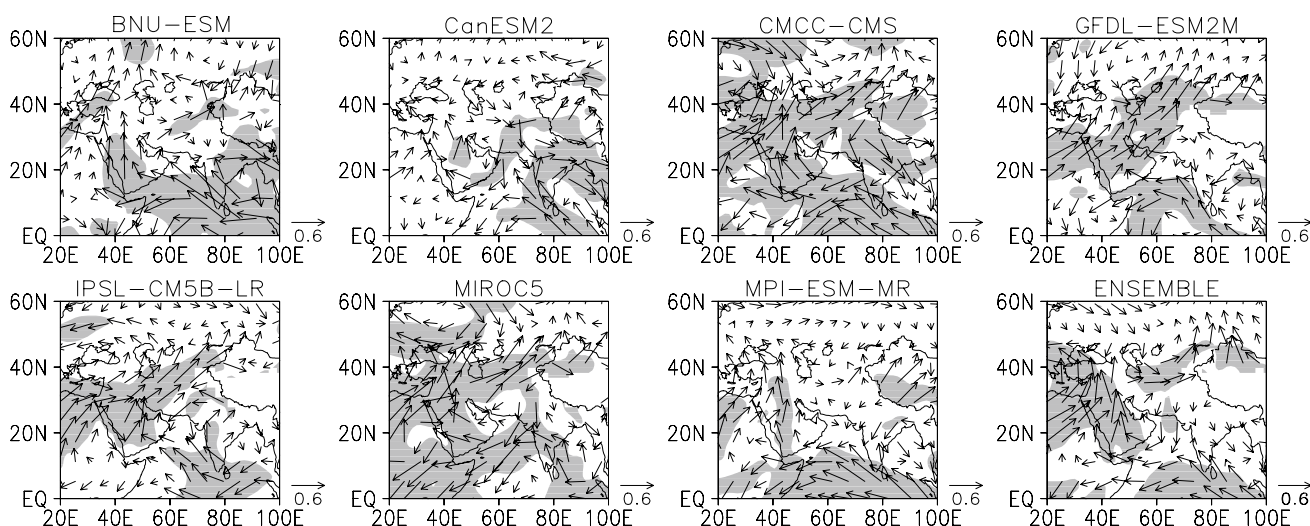
Fig. 7 Correlations between regionally averaged SSTs over the domain of 50–75°E, 5–25°N and horizontal wind averaged between 850 and 700 hPa in seven selected models (see text for details).

Shaded regions present over 95 % significant level. The last panel is the 7-model ensemble averages

rainfall climatology received. Most of the changes here are more than 50 % of their corresponding seasonal means (not shown). MPI-ESM-MR is the only model showing overall rainfall reduction in most of the region. Despite of the fact that area-averaged results in Fig. 8 suggest CMCC-CMS simulates rainfall reduction, it actually has rainfall increases over part of the northwest China.

For the seven models which have shown their reasonable skills in modeling the influence of SSTs in the Arabian Sea on the summer rainfall over CA, the dynamical processes leading to such rainfall increases are also consistent with each other. By and large, they all show (Fig. 11) that SSTs warming in the Arabian Sea and tropical IO is associated with an anti-cyclonic flow pattern in the region. The enhanced southerly flow brings warm and moist air up further north into the CA region. For the MIROC5 model, although it simulates an anti-cyclonic flow pattern in the Arabian Sea and western part of the IO, a cyclonic flow dominates over the Bay of Bengal and this flow prevents the southwest flow over the Arabian Sea penetrating further northeastward. As a result, in this model, summer rainfall increases are limited in lower latitudes than in other models. Note that for the two models (CMCC-CMS and MPI-ESM-MR) with averaged rainfall decreases over CA in Fig. 8b, the enhanced southerly flow can also be seen in part of the region. Therefore, there may be other important factors of rainfall generation in these models over CA which offsets the effect of enhanced moisture source from the tropics and leads to a weak rainfall reduction in the region. Within the context of our analysis, we are not able to explore this further to discuss the exact causes of such detailed inter-model differences.

Nevertheless, based on our detailed process-based analysis by comparing observed and model-simulated processes influencing the summer rainfall in CA, our confidence is enhanced that under global warming, the CA is likely to receive more summer rainfall due to the dynamical and moisture transport processes demonstrated in these skillful models.

Overall results in this section demonstrate the importance of analyzing the underlying physical/dynamical processes in the climate models when deriving regional climate change projections. It is possible one model may give a good rainfall climatology or simulate a good rainfall correlations with SSTs or other important climate drivers, but such results do not necessarily mean the underlying processes supporting such results are realistic in these models. Therefore, results from this study question the selection of models based on their rainfall/temperature climatology alone.

As described in Sect. 2, to complement the analysis presented above, in this study, we have further conducted four SST sensitivity experiments using a local climate model named ACCESS1.3 which also participated in CMIP5. The differences between ACCESS-rcp85 and ACCESS-his represent the climate changes with warmed global SSTs and increased atmospheric greenhouse concentration. Similarly, the differences between ACCESS-onlyIO and ACCESS-his represent the changes caused by warmed IO and increased atmospheric greenhouse concentration. In contrast, the differences between ACCESS-no IO and ACCESS-his reflect the changes caused by increased atmospheric greenhouse concentration but no IO SST warming. Finally, the difference between ACCESS-onlyIO and ACCESS-no IO can be
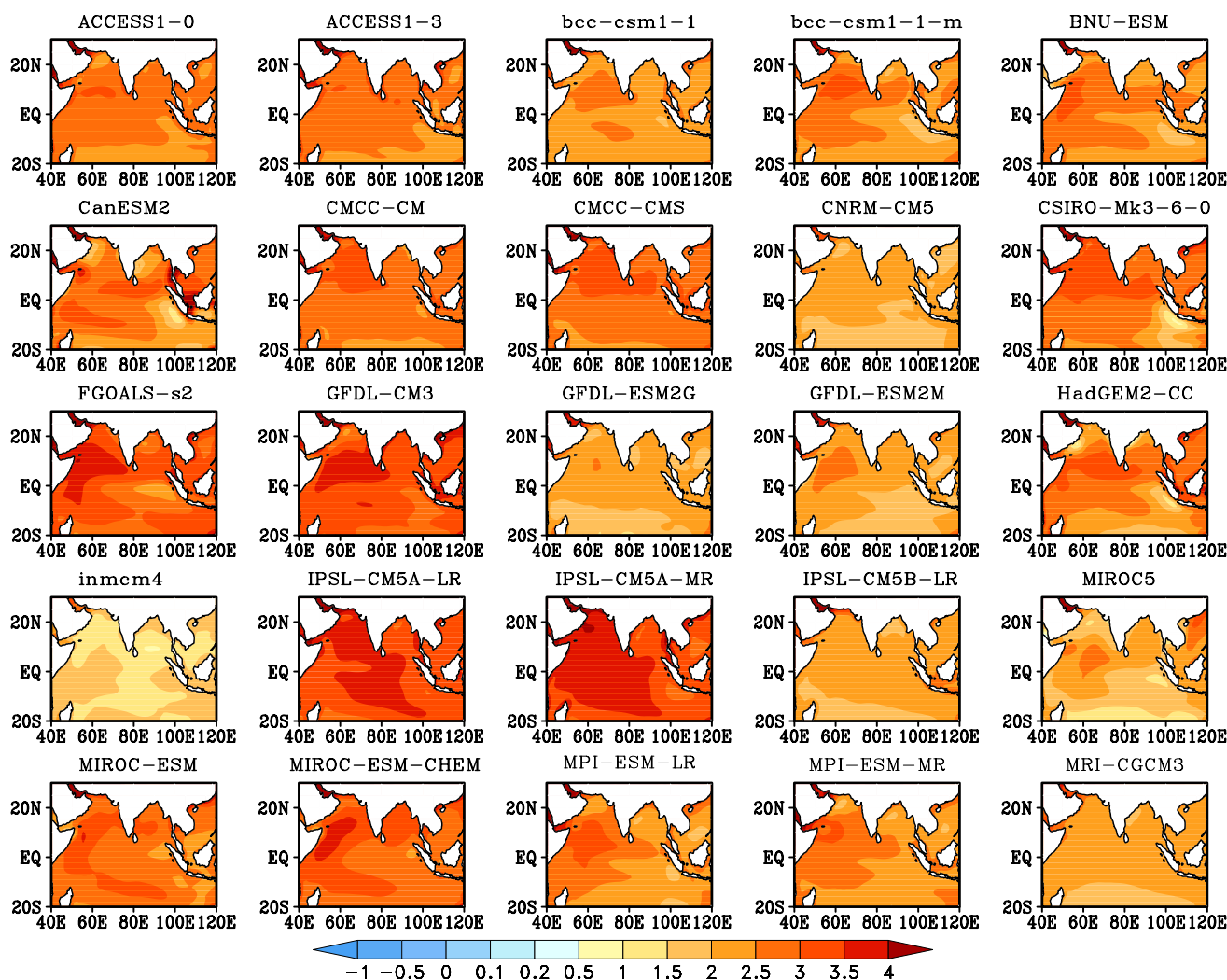
Fig. 8 Changes in SSTs (°C, 2051–2100 minus 1961–2004) in JJA over Indian Ocean by 25 CMIP5 models

attributed to the influence of IO warming on the regional climate projections.

Figure 12a shows the seasonal evolution of monthly rainfall changes averaged over the longitudinal band of 65–95°E between the four sets of experiments. In Fig. 12a, with the increases in greenhouse gas concentrations and globally warmed SSTs, the model displays a reduction in tropical summer monsoon rainfall over the latitudes of 0–20°N during the April to August period. To its north, there is a weak rainfall increase. If only superimposing the warming in the IO (without SST warming in other ocean basins), the model results in Fig. 12b not only suggest a much broader and more enhanced rainfall increases in the tropical domain, but the rainfall increases are expanded further northward into the middle latitudes, up to 35°N in July–August-September. In contrast, without the IO warming (but SST warms over other ocean basins), the whole tropical latitudinal band is dominated by rainfall decreases and

the rainfall decreases extending up to the latitudes around 30°N (Fig. 12c). By calculating the differences between ACCESS-onlyIO and ACCESS-no IO, Fig. 12d shows that the IO SST warming leads to the rainfall increases in the tropics and extending further northward to 30–35°N. In addition, over the central Asian domain latitudinal band (35–60°N), along the increase in tropical monsoon rainfall, a rainfall increase is clearly presented in Fig. 12d. This modeling results suggest that IO SST warming is an important factor leading to rainfall increases in CA. Note that rainfall is reduced (along the band of 30–40°N during May to August period) between the increases in tropics and the increases in CA in Fig. 12d. This can be explained by the enhanced subtropical descending motion as discussed in Figs. 2a and 7 in which we see enhanced tropical Indian monsoon tend to lead to enhanced anti-cyclonic circulation to its north in the subtropical region. This is also consistent with the two-step moisture transport mechanism discussed
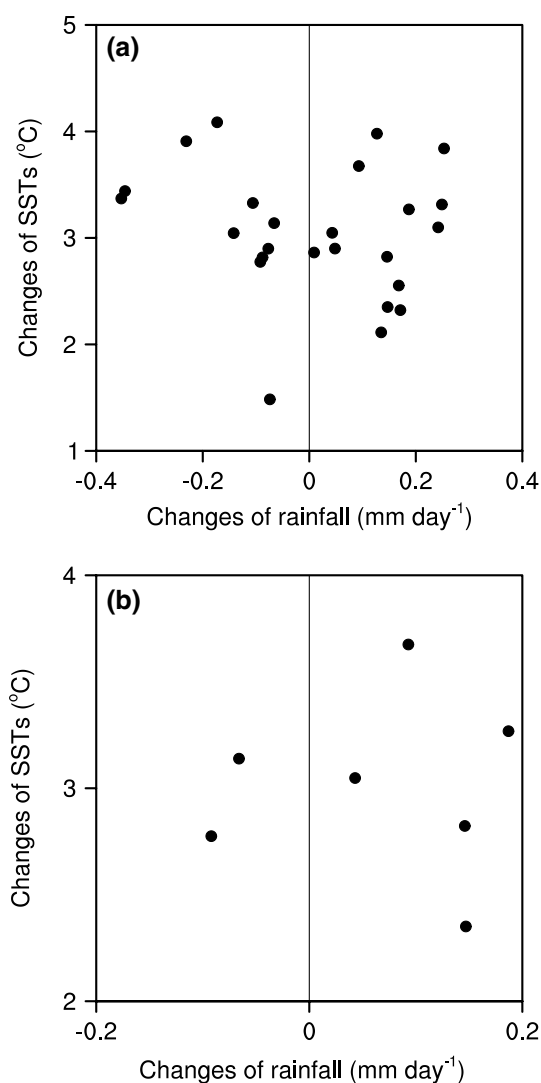
Fig. 9 a Scatter plots of the changes in regionally averaged rainfall (mm day^{-1}, 2051–2100 minus 1961–2004) from the domain of 65–95°E, 35–50°N in x-axis and regionally averaged SSTs (°C, 2051–2100 minus 1961–2004) from the domain of 50–75°E, 5–25°N in y-axis in 25 models, **b** as **a** but for seven selected models

in Sect. 3, with the rainfall increases in CA being an indirect consequence of tropical monsoon variations responding to tropical SST forcing.

Furthermore, several pieces of additional information can be obtained from these particular modeling results in Fig. 12. (1) IO SST warming is a driving force for the atmospheric circulation variations, rather than a passive response to regional atmospheric circulation variations caused by the forcing outside of the IO domain (i.e. tropical Pacific SSTs). Warmed IO SSTs enhances the Indian monsoon and its cyclonic circulation pattern in the tropics; (2) Without the IO warming, much warmed SSTs over tropical central Pacific Ocean (with an El Nino-like SST warming pattern) could lead to significant rainfall decreases in the

IO basin (Fig. 12c). The IO warming therefore acts to offset a large part of such influence from the tropical Pacific; (3) It is well known Indian monsoon is generally weak in climate models including ACCESS1.3. In particular, they tend to lack of northward penetration of monsoon rainfall into the Indian subcontinent. Several studies have suggested cooling biases in the Arabian Sea (e.g., Levine et al. 2012) contributed to such modeling results. Our experiments here also tend to support this claim as IO warming in this model leads to enhanced tropical monsoon rainfall and its northward penetration. Although ACCESS1.3 is not part of the seven models selected in this analysis, with a weak Indian monsoon in its climate simulations (Bi et al. 2013), the processes identified in this model's SST experiments here are still valid for complementing our CMIP5 model analysis. In future studies, we plan to further examine the processes revealed here using a different model and with more carefully designed SST experiments (such as separating the SST warming in the Arabian Sea and the Bay of Bengal).

5 Conclusion and discussions

Rainfall is very low over CA. Thus, small rainfall changes in this region can have significant social, economic, and ecological consequences. Existing studies showed that one of the most important social and political risks associated with climate change pertains to water availability, especially over CA (Dinar and Dinar 2003; Wolf et al. 2003). So understanding the variations of rainfall in the region in future warmed climate became very important. Nevertheless, large uncertainty exists in current climate model projected change in rainfall over CA (Huang et al. 2013). In this study, we have focused on exploring the impacts of IO warming on the summer rainfall over CA.

In recent decades, SSTs over the IO become warmer, especially in the Arabian Sea (Chambers et al. 1999; Roxy et al. 2014). Meanwhile, rainfall also has experienced an increased trend over CA (Chen et al. 2011). Some observational studies suggested that summer rainfall over CA could be closely related to the SST anomalies in IO, with moist air being transported to CA under suitable circulations (Yang et al. 2010; Bothe et al. 2012; Zhao et al. 2014; Zhou et al. 2015). In order to confirm the relationship, we have firstly analyzed the correlations between the summer rainfall over CA and SSTs in IO in 25 CMIP5 models in their *historical* experiments for the period of 1961–2004. After that, we have explored the dynamical processes leading to the impact of SST warming in the Arabian Sea on the projected change of summer rainfall over CA in the second half of twenty-first century in these models *RCP8.5* experiments. Furthermore, we have conducted ACCESS1.3 SST sensitivity experiments to re-examine the processes derived from the CMIP5 models.
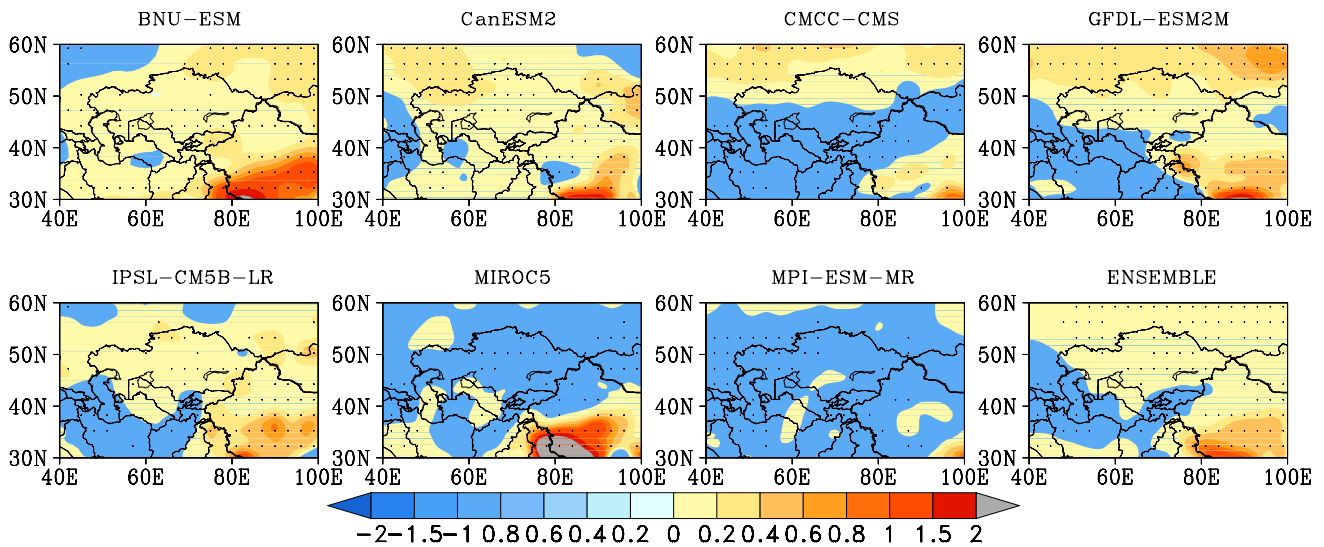
Fig. 10 Changes in summer rainfall (mm day^{-1}, 2051–2100 minus 1961–2004) over central Asia by seven selected models. The last panel is the seven-model ensemble averages
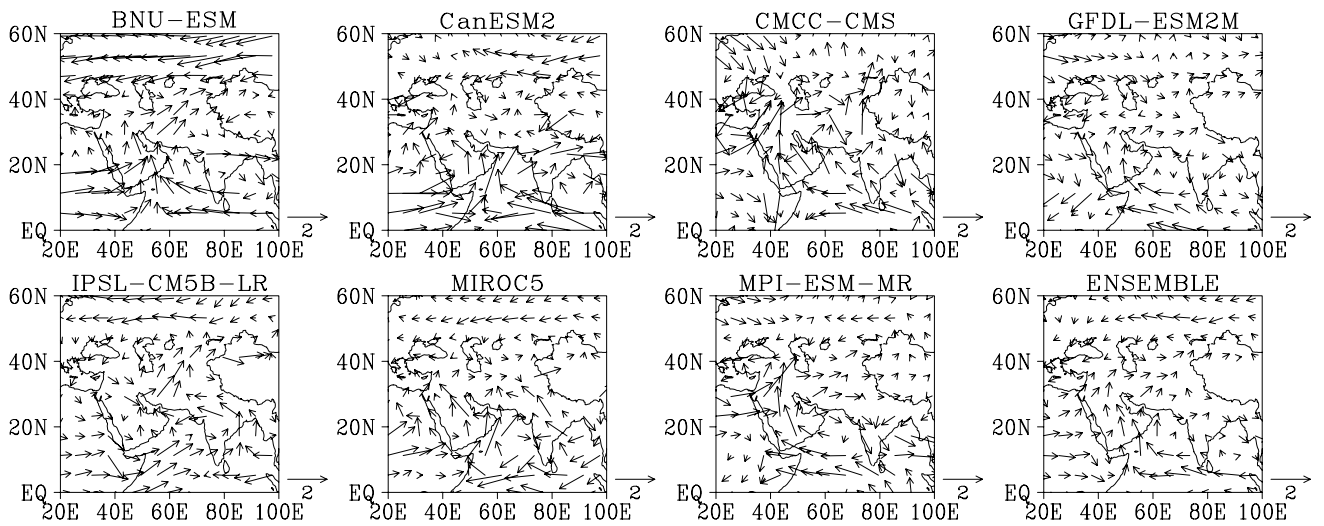

Fig. 11 Changes in horizontal wind averaged between 850 and 700 hPa (m s^{-1}, 2051–2100 minus 1961–2004) in summer by seven selected models. The last panel is the seven-model ensemble averages

Correlation analysis with observational data shows that summer rainfall is well correlated to the SSTs in northern IO. This is largely contributed to the two-step moisture transport process as discussed in Zhao et al. (2014). While a majority of the CMIP5 models show similar correlations as observed, the magnitude of the correlations varies significantly across the models. Furthermore, most models tend to show that the SST anomalies in the Arabian Sea have higher correlations than ones in the Bay of Bengal. Thus in the analysis we have concentrated on the impacts of the SSTs warming in the Arabian Sea.

Based on the correlation analysis, we have selected seven out of the total 25 models with relative better

statistical relationships between CA rainfall with IO SSTs and regional circulation connections with IO SSTs as revealed by observational analysis. Most of the models can capture the observed circulation features associated with summer rainfall over CA (Yang and Zhang 2007; Zhao et al. 2014) and SSTs in IO. In these models, the SST warming in the Arabian Sea is favourable for an enhanced southerly flow over the west part of the IO which transports warm and moist air from the IO into the lower lands between the Iranian Plateau and the Tibetan Plateau. At the same time, there is a cyclonic circulation pattern over CA which brings these moist air masses further north into the CA region.

Fig. 12 a Zonally averaged (65–95°E) changes in monthly rainfall between ACCESS-rcp85 and ACCESS-his SST experiments (mm day^{-1}). See text in Sect. 2 for experimental details, **b** as **a** but for ACCESS-only IO and ACCESS-his, **c** as **a** but for ACCESS-no IO and ACCESS-his, **d** as **a** but for ACCESS-only IO and ACCESS-no IO
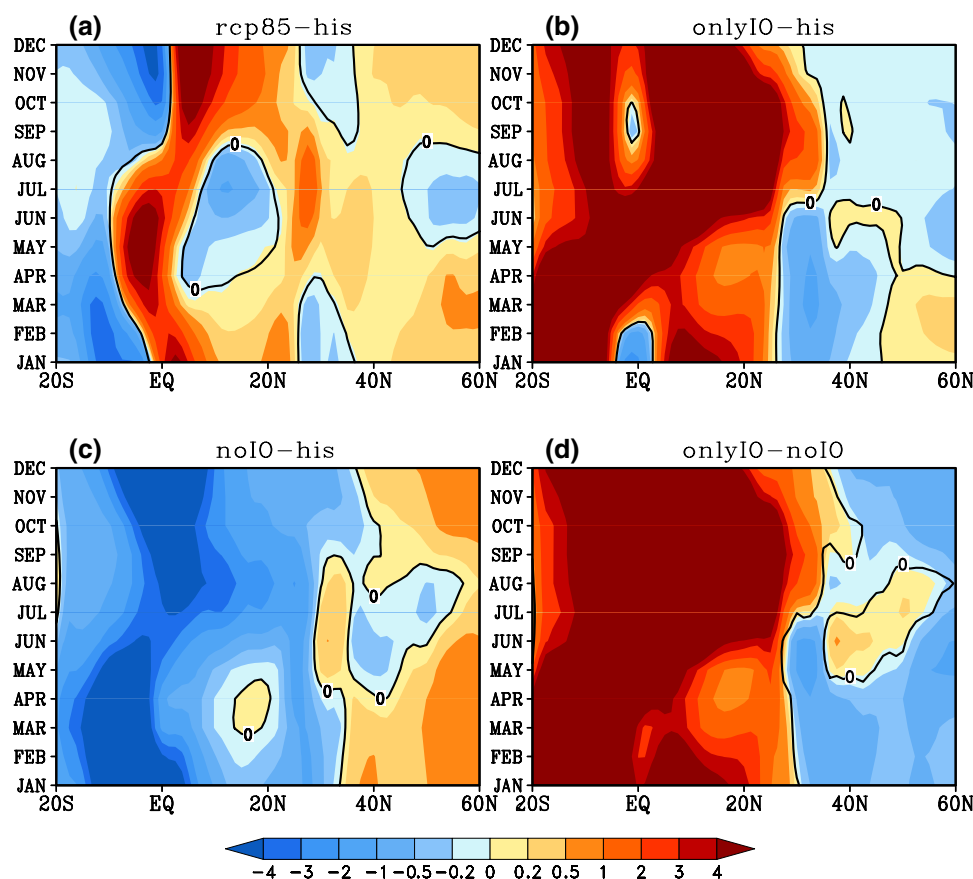
Our results also showed that under global warming, the SSTs in the Arabian Sea increase in all the 25 models, but the changes of summer rainfall over CA present remarkable differences. Of the 25 models, about 14 of them projected rainfall increases in CA while the rest 11 models projected the opposite changes. When using the seven models objectively selected based on their skills in capturing the influence of IO on CA rainfall, the uncertainties are largely reduced: five out of the seven models suggested the rainfall will increase over CA under warmed climate. Above result confirms the importance of exploring and understanding physical mechanisms presented in the climate models when deriving future rainfall changes at region scale. Results from our SST sensitivity experiments further support our claims. The four sets of ACCESS1.3 experiments have shown that IO SST warming is favourable for the enhanced tropical Indian monsoon and its northward penetration.

Yet, there are several weaknesses in our analysis. In the current study we only focused on the Arabian Sea because it was highly correlated to the summer rainfall over CA. We don't distinguish it from the effects caused by SSTs gradients in the Arabian Sea and Bay of Bengal. In addition, the SST warming is a global phenomenon. Besides the Arabian Sea, the SSTs in north Atlantic and the warm pool of northwest Pacific are also related to the summer rainfall over CA (Yang et al. 2010). Although we have conducted

ACCESS1.3 SST experiments as our first attempt to separate such impacts, it is likely that such results may be model dependent. Further work is need to confirm such results using different climate models and with more carefully designed experiments. It is well known land–air coupling is another important processes in the CA climate, with modelling studies from Koster et al. (2004) showing a strong land-air coupling in this region. We have not explored the issue that to what extent the uncertainty in these model projections are also caused by different land-surface processes in current and future climate. All these will be pursued in our further studies.

References

Alory G, Wijffels S, Meyers G (2007) Observed temperature trends in the Indian Ocean over 1960–1999 and associated mechanisms. Geophys Res Lett 34:L02606. doi:10.1029/2006GL028044

Ashok K, Guan Z, Yamagata T (2001) Impact of the Indian Ocean dipole on the relationship between the Indian monsoon rainfall and ENSO. Geophys Res Lett 28:4499–4502

Bi D et al (2013) The ACCESS coupled model: description, control climate and preliminary validation. Aust Meteorol Oceanogr J 63:41–64

Bothe O, Fraedrich K, Zhu X (2012) Precipitation climate of central Asia and the large-scale atmospheric circulation. Theor Appl Climatol 108:345–354

Chambers D, Tapley B, Stewart R (1999) Anomalous warming in the Indian Ocean coincident with El Nino. J Geophys Res 104:3035–3047

Chen FH, Wang J, Jin L, Zhang Q, Li J, Chen J (2009) Rapid warming in mid-latitude central Asia for the past 100 years (in Chinese). Front Earth Sci 3:42–50

Chen FH, Huang W, Jin L, Chen J, Wang J (2011) Spatiotemporal precipitation variations in the arid central Asia in the context of global warming (in Chinese). Chin Earth Sci 54:1812–1821

Clark CO, Cole J, Webster P (2000) Indian Ocean SST and Indian summer rainfall: predictive relationships and their decadal variability. J Clim 13:2503–2519

Dinar S, Dinar A (2003) Recent developments in the literature on conflict negotiation and cooperation over shared international fresh waters. J Nat Resour 43:1217–1286

Dong G, Zhang H, Moise A, Hanson L, Liang P, Ye H (2015) CMIP5 model-simulated onset, duration and intensity of the Asian summer monsoon in current and future climate. Clim Dyn. doi:10.1007/s00382-015-2588-z

Du Y, Xie SP (2008) Role of atmospheric adjustments in the tropical Indian Ocean warming during the 20th century in climate models. Geophys Res Lett 35:L08712. doi:10.1029/2008GL033631

England MH, Ummenhofer C, Santoso A (2006) Interannual rainfall extremes over southwest Western Australia linked to Indian Ocean climate variability. J Clim 19:1948–1969

Fan FX, Mann ME, Lee S, Evans JL (2010) Observed and model changes in the south Asian summer monsoon over the historical period. J Clim 23:5193–5205

Fan FX, Mann ME, Lee S, Evans JL (2012) Future changes in the south Asian summer monsoon: an analysis of the CMIP3. J Clim 25:3909–3928

Giannini A, Saravanan R, Chang P (2003) Oceanic forcing of Sahel rainfall on interannual to interdecadal time scales. Science 302:1027–1030

Gille ST (2002) Warming of the Southern Ocean since the 1950s. Science 295:1275–1277

Hoerling M, Hurrell JW, Xu T, Bates GT, Phillips AS (2004) Twentieth century North Atlantic climate change part II: understanding the effect of Indian Ocean warming. Clim Dyn 23:391–405

Houghton JT, Ding YH, Griggs DJ, Noguer M, van der Linden PJ, Dai X, Maskell K, Johnson CA (eds) (2001) Climate change 2001: the scientific basis. Cambridge University Press, Cambridge

Huang JP, Guan X, Ji F (2012) Enhanced cold-season warming in semi-arid regions. Atmos Chem Phys 12:5391–5398

Huang DQ, Zhu J, Zhang YC, Huang AN (2013) Uncertainties on the simulated Summer precipitation over Eastern China from the CMIP5 models. J Geophys Res Atmos 118:9035–9047

Huang AN, Zhou Y, Zhang YC, Huang DQ, Zhao Y, Wu HW (2014) Changes of the annual precipitation over central Asia in the twenty-first century projected by multi-models of CMIP5. J Clim 27:6627–6646

Huxman TE, Smith SD (2001) Photosynthesis in an invasive grass and native for bat elevated CO$_2$ during an El Nino year in the Mojave Desert. Oecologia 128:193–201

Jone PD, Osborn TJ, Briffa KR (2001) The evolution of climate over the last millennium. Science 292:662–667

Kalnay E et al (1996) The NCEP/NCAR 40-year reanalysis project. Bull Am Meteorol Soc 77:437–471

Kawamura R (1994) A rotated EOF analysis of global sea surface temperature variability with interannual and interdecadal time scales. J Phys Ocean 24:707–715

Koster RD et al (2004) Regions of strong coupling between soil moisture and precipitation. Science 305:1138–1140

Lau KM, Weng HY (1999) Interannual, decadal-interdecadal, and global warming signals in sea surface temperature during 1955–97. J Clim 12:1257–1267

Levine RC, Turner AG, Marathayil D, Martin GM (2012) The role of northern Arabian Sea surface temperature biases in CMIP5 model simulations and future projections of Indian summer monsoon rainfall. Clim Dyn 41:155–172

Levitus S, Antonov J, Boyer T (2005) Warming of the world ocean. Geophys Res Lett 32:L02604. doi:10.1029/2004GL021592

Lioubimtseva E, Cole R, Adams JM, Kapustin G (2005) Impacts of climate and land-coverchanges in arid lands of central Asia. J Arid Environ 62:285–308

Mariotti A, Ballabrera-Poy J, Zeng N (2005) Tropical influence on Euro-Asian autumn rainfall variability. Clim Dyn 24:511–521

Mason SJ, Goddard L (2001) Probabilistic precipitation anomalies associated with ENSO. Bull Am Meteorol Soc 82:619–638

Mitchell TD, Jones PD (2005) An improved method of constructing a database of Monthly climate observations and associated high-resolution grids. Int J Climatol 25:693–712

Reynolds RW, Rayner NA, Smith TM, Stokes DC, Wang W (2002) An improved in situ and satellite SST analysis for climate. J Clim 15:1609–1625

Roxy MK, Ritika K, Terray P (2014) The curious case of Indian Ocean warming. J Clim 27:8501–8509

Shi YF, Shen YP, Hu RJ (2002) Preliminary study on signal, impact and foreground of climatic shift from warm-dry to warm-humid in Northwest China (in Chinese). J Glaciol Geocryol 24:219–226

Solomon S, Qin DH, Manning M, Chen Z, Marquis M, Averyt KB, Ignore M, Miller HL (eds) (2007) Climate change 2007: the physical science basis. Cambridge University Press, Cambridge

Sooraj KP, Terray P, Mujumdar M (2014) Global warming and the weakening of the Asian summer monsoon circulation: assessments from the CMIP5 models. Clim Dyn. doi:10.1007/s00382-014-2257-7

Taylor KE, Stouffer RJ, Meehl GA (2012) An overview of CMIP5 and the experiment design. Bull Am Meteorol Soc 93:485–498

Uppala SM et al (2005) The ERA-40 re-analysis. Q J R Meteorol Soc 131:2961–3012

Whitford W (2002) Ecology of desert systems. Academic Press, San Diego

Wolf AT, Yoffe SB, Giordano M (2003) International waters: identifying basins at risk. Water Policy 5:29–60

Wu HW, Huang AN, He Q, Zhao Y (2013) Projection of the spatial and temporal variation characteristics of precipitation over central Asia of 10 CMIP5 models in the next 50 years (in Chinese). Arid Land Geogr 36:669–679

Xu ZF, Qian YF (2006) Moist potential vorticity index of Indian monsoon and its relationship with climate in China (in Chinese). Acta Meteorol Sin 64:760–769

Yang LM, Zhang QY (2007) Circulation characteristics of interannual and Interdecandal anomalies of summer rainfall in north Xinjiang (in Chinese). Chin J Geophys 50:412–419

Yang LM, Xiao KT, Zhang QY (2009) Relationships between rainfall anomalies in Xinjiang summer and Indian rainfall (in Chinese). Plateau Meteorol 28:564–572

Yang LM, Yang T, Zhao L, Wang MZ (2010) Relationship between summer precipitation in northern Xinjiang and sea surface temperature anomalies (in Chinese). J Desert Res 30:1215–1220

Zeng ZM, Yan Z, Ye DZ (2001) The regions with the most significant temperature trends during the last century. Adv Atmos Sci 18:481–496

Zhang JB, Deng ZF (1987) A conspectus of precipitation in Xinjiang. Meteorological Press, Beijing, pp 113–117

Zhang YH, Yang LM, Xiao KT, Qin H, Li YY, Yang X (2012) The central Asian vortexes activity during 1971–2010 (in Chinese). J Appl Meteorol Sci 23(3):312–321

Zhang H, Dong G, Moise A, Colman R. Hanson L, Ye H (2015) Uncertainty in CMIP5 model-projected changes in the onset/retreat of the Australian summer monsoon. Clim Dyn. doi:10.1007/s00382-015-2707-x

Zhao Y et al (2014) Impact of the middle and upper troposphere cooling over central Asia on the summer rainfall in the Tarim Basin, China. J Clim 27:4721–4732

Zhou Y, Huang AN, Zhao Y, Yang Q, Jiang J, La M (2015) Influence of the sea surface temperature anomaly over the Indian Ocean in March on the summer rainfall in Xinjiang. Theor Appl Climatol 119:781–789